Title: Effects of Shifting Snowmelt Regimes on the Hydrology of Non-Alpine Temperate Landscapes

Author Names and Affiliation: Chanse M. Ford[1], Anthony D. Kendall[1], David W. Hyndman[1]

[1]Department of Earth and Environmental Science, Michigan State University, East Lansing, MI, USA

Corresponding Author: Chanse Ford

Address:

Department of Earth and Environmental Science

Natural Science Building

288 Farm Lane, Room 207

East Lansing, MI 48824

Email: fordchan@msu.edu

Phone: (517) 355-4626

Keywords: Snowmelt hydrology; Great Lakes; climate change; Michigan

1. Introduction

High-latitude, temperate, low elevation regions around the globe depend on seasonal snowfall for a significant portion of their annual water budgets. While cryosphere research has generally focused on alpine and arctic regions, changing climate conditions are already affecting snow hydrology across vast but relatively understudied regions (Burakowski et al., 2008; Hodgkins and Dudley, 2006a; Huntington et al., 2004; Javed et al., 2019; Suriano et al., 2019). Indeed, the comparatively low-relief topography characteristic of the non-alpine, non-arctic cold regions of the world make large areas particularly sensitive to the effects of shifting patterns of snow accumulation and melt (Clark et al., 2011). In particular, these regions are moving from relatively persistent seasonal snowpack to a thinner snowpack and increased bare ground days (Suriano and Leathers, 2017). The hydrologic effects of this regime shift are not well understood, but will reshape economies, ecosystems, water resources, and the needs of built infrastructure during the coming decades (Chin et al., 2018; Suriano et al., 2019; Zou et al., 2018).

Snowpack and melt research in recent decades has primarily focused on the mountainous regions of the western United States, Europe, and Asia. Many studies have examined the potential effects of global climate change on alpine snowpacks and subsequently on mountain streamflow. Studies of historical trends in snow accumulation and melt in the western United States have shown declining snowpack thicknesses, earlier melting, and more winter/spring precipitation occurring as rain rather than snow over recent decades (Clow, 2010; Hamlet et al., 2005; Jefferson et al., 2008; Mote, 2003; Stewart et al., 2004). These trends are not limited to the alpine areas of the country.

Several regional studies have found similar historical snow trends in the central and eastern U.S. (Burakowski et al., 2008; Hodgkins and Dudley, 2006a; Huntington et al., 2004), including reduced snow cover, lower snow to total precipitation ratios (S/P) and more melting in winter months rather than the traditional late Spring melt (Dyer and Mote, 2006; Feng and Hu, 2007; McCabe and Wolock, 2009; Suriano and Leathers, 2017; Suriano et al., 2019). Future climate scenarios continue to project decreased snow with earlier melting (Adam et al., 2009; Barnett et al., 2005; Boyer et al., 2010; Campbell et al., 2011; Chin et al., 2018; Demaria et al., 2016; Hayhoe et al., 2007; Hayhoe et al., 2010; Mortsch et al., 2000; Peacock, 2012).

The hydrologic effects of these melt changes have been observed in alpine settings of the western U.S., including lower peak flows that occur earlier in the season, and earlier overall streamflow regimes including earlier center of streamflow volume arrival times (Clow, 2010; Hidalgo et al., 2009; Jefferson et al., 2008; Stewart et al., 2009). Similar observations of spring streamflow have been made in the eastern half of the country (including the Great Lakes), but to a lesser degree (Hodgkins and Dudley, 2006b; Hodgkins et al., 2007; Huntington et al., 2004; Javed et al., 2019; Johnson and Stefan, 2006; Johnston and Shmagin, 2008). As the warming associated with global change progresses, the expectation is that streamflow will continue to shift earlier in the year across the globe (Arora and Boer, 2001; Barnett et al., 2005; Berghuijs et al., 2014; Boyer et al., 2010; Brubaker and Rango, 1996; Byun and Hamlet, 2018; Campbell et al., 2011; Champagne et al., 2020; Cherkauer and Sinha, 2010; Hayhoe et al., 2007; Mortsch et al., 2000; Tu, 2009). As such hydrologic changes become more pronounced and widespread, it will be critical for research to be conducted on the snowmelt hydrology of lesser studied regions of the planet, including the often-overlooked groundwater component of the hydrologic cycle.

Here we focus on the Laurentian Great Lakes region of North America (hereafter "Great Lakes"), and in particular the state of Michigan, USA. Situated in the midst of four Great Lakes, Michigan is geographically unique, and serves as a mesocosm for high-latitude temperate climate regions globally. The range of snowfall across the state, both due to its latitudinal extent and the "Lake Effect" phenomenon, encompasses nearly the entire range for the continental US; some areas within the state receive less than 100 mm SWE of snowfall, while the northern regions typically receive just over half a meter in a year (Fig. 1a). Michigan also has remarkable hydrogeologic diversity for its area, spanning 12 of the 20 US Hydrologic Land Regions (Wolock et al., 2004), with soils spanning the range from heavy clay to coarse sand.

Despite the importance of snow to Great Lakes annual water budgets, and the potential negative consequences of changes to the typical snowmelt regime, research into snowmelt patterns across this region has been limited. Within the Great Lakes region, relatively few studies have examined historical snowmelt trends. Hodgkins et al. (2007) found that from 1955-2004 snowmelt occurred earlier in the year with decreasing S/P ratios. Most climate model simulations of the Great Lakes region show increases in winter and spring precipitation, however warmer temperatures will lead to more rain and less snow (Hayhoe et al., 2010). Historical data from the last century in this region shows that as climate warmed, annual precipitation amounts have increased, leading to increased streamflow (Hodgkins et al., 2007). The relation of this increased precipitation to streamflow from historical data remains unclear, as early spring precipitation typically decreased over the last 50 years, but total runoff (sum of surface and groundwater components) increased, indicating earlier melting and more precipitation falling as rain. The decrease in amount of runoff from melt corresponded with flow peaks earlier in the season, decreased peak streamflows, and earlier peak Great Lakes levels (Argyilan and Forman, 2003; Johnson and Stefan, 2006; Novotony and Stefan, 2007). Those studies analyzed changes to the hydrologic cycle focused on a specific drainage basin (or similar scales). Where studies have taken a broader spatial perspective, they have generally focused on analyzing just one component of the hydrologic cycle. Here, we seek to holistically examine how changing snowmelt dynamics are affecting the broader hydrologic cycle over a large non-alpine region.

To best understand the potential snowmelt hydrology changes, taking into account differences in climate, land use, geology and hydrology across Michigan, we quantify changes to seasonal snowmelt and the influence it has on groundwater recharge and streamflow. Anecdotally, Michigan's seasonal snowpack in Michigan in recent years appears to have deviated from the historically "typical" season-long persistence, instead melting periodically throughout the winter months. We hypothesize that: 1) warmer winters have led to less snowmelt, and 2) reduced snowpack persistence, typified by earlier melt and more bare ground days throughout the winter, leading to 3) earlier and lower spring peak flow in streams, and 4) increased recharge of shallow groundwater. This paper examines these four linked hypotheses by first categorizing recent years as "warm" or "cool" based on a multimetric analysis of different winter temperature parameters across Michigan's substantial north-south climate gradient. We leverage 14 years of gridded, assimilated model data of snowpack and melt to quantify differences across this gradient between warm and cool years. Finally, we correlate these changes with variations in drainage basin hydrology across year types.

2. Methods

2.1 Study Region

Although the high-latitude Midwestern United States, particularly the Great Lakes region, is neither arctic nor alpine it still receives a significant portion of its water budget from seasonal snowfall. Some of the highest annual snowfall totals in the eastern half of the United States occur in this region. In the Upper Peninsula (UP) of Michigan, annual snow water equivalence totals can exceed half a meter (Figure 1a, and Andresen, 2012).

Impacts of warming winter temperatures due to global climate change on Michigan's winter hydrology are unclear. Climate projections for Michigan show an increase in annual precipitation, but it is not clear how much of that precipitation will occur as snow (Hayhoe et al., 2010); even in areas where annual snowpack thickness has been increasing, the number of days with snow covered ground appears to be decreasing (Andresen, 2012). Fewer days with snow on the ground would indicate a shift in the melt regime of the snowpack, in turn altering recharge and spring streamflow amounts.

Michigan's geology changes along a north-south gradient due to numerous glacial advances and retreats during the last ice age (Supplementary Fig. 1; Farrand and Bell, 1992; Groundwater Inventory and Mapping Project, 2003). The shallow sediments and aquifers in the LP are dominantly sands to sandy loams, which are mostly underlain by sedimentary bedrock. In contrast, the UP has shallow soils underlain by less permeable Precambrian igneous formations. As a result, it has distinctly different hydrology that is more dominated by surface flow than subsurface flows.

Michigan's also has a strong land use gradient from north to south. The southern portion is predominantly agricultural, growing the same variety of staple crops seen throughout the rest of the U.S. Midwest: corn, soybeans, alfalfa and hay crops are some of the primary agricultural outputs of the region (Hamlin et al., 2020; Homer et al., 2004; 2015; Supplementary Figure 1). Most of the state's major urban centers are also in the south, creating a landscape of urbanized areas surrounded by intensively managed farmlands. By contrast the state's northern Lower Peninsula (NLP) and Upper Peninsula (UP) are dominated by mixed and coniferous forests with less urban and agricultural land than the southern portion.

There are distinct precipitation patterns across Michigan, largely due to the "Lake Effect" phenomenon (Fig. 1). The LP's climate is strongly influenced by winds that come from the north- to the south-west across Lake Michigan (Andresen, 2012). As the air moves over the large lake, water vapor content increases due to evaporation. Shortly after these air packages reach land, this additional water vapor commonly condenses, producing substantially more precipitation on the western portion and northern tip of the peninsula. Average annual snow water equivalent (SWE) totals across the LP range from < 200 mm in the southeastern LP to >400 mm in the northern part. The UP's precipitation patterns are similarly affected by Lake Superior. The northern parts of the UP can receive very heavy snowfall, with an average annual SWE of up to ~ 0.5 meter.

To best understand potential snowmelt hydrology changes, taking into account differences in climate, land use, geology and hydrology, the state was divided into three regions (Fig. 1). The UP, with its high wetland and forested fraction and distinct hydrogeology was assigned as one region. The LP was split in two (Northern Lower Peninsula, NLP, and Southern Lower Peninsula, SLP), with the dividing line of approximately 43.8° N latitude chosen because it best divides the LP based on geologic, land use, and climatic differences. Using these regional delineations, snowmelt patterns and hydrologic responses were analyzed between the 2004 to 2017 water years.

2.2 Data Sources

We combined observations and model-data reanalysis from several sources. Daily temperature and precipitation data from weather stations were extracted from the Global Historical Climatology Network (GHCN) (Menne *et al.* 2012). Daily snowpack SWE and melt values were derived from the National Oceanic and Atmospheric Administration's (NOAA)

Snow Data Assimilation (SNODAS) model (NOHRSC, 2004). Stream gauge daily average flow data came from the U.S. Geological Survey's (USGS) stream gauge network (USGS, 2018). Daily precipitation and average temperature values were extracted from the PRISM reanalysis data (PRISM Climate Group, 2018). All datasets were analyzed from October 2003 to June 2017.

All GHCN and USGS gauges within the three study subregions were included, provided that 95% of the total daily observations across "snow seasons" (defined here as October 1 through May 31 of the following year) were present. With this constraint, maximum and minimum daily air temperature were available from 240 weather stations. Mean air temperature for each day was calculated as the arithmetic mean of the provided maximum and minimum daily temperatures. Daily streamflow data were available from 123 USGS stream gauging stations.

The output from NOAA's SNODAS model was one of the primary input sources for this study. SNODAS is a data assimilation model that is calibrated to snow and climate observation data (Barrett, 2003); it performs well, particularly in areas with relatively low relief (Clow et al., 2012; Hedrick et al., 2015). SNODAS uses downscaled outputs from numerical weather prediction models in conjunction with empirical meteorological data from airborne and ground-based weather stations along with satellite data to model snow across the continental United States. The model outputs daily 1-kilometer grids of snowpack thickness and temperature, along with other simulated snowpack properties such as daily melt, across the conterminous United States. The model output first became available in early 2003, which is thus the beginning date for our analysis period. We used the outputs of modeled snowpack SWE and melt from the base of the snowpack.

The non-snow precipitation data came from the PRISM model (PRISM Climate Group, 2018). This model outputs daily 4-kilometer gridded interpolations of total precipitation, minimum and maximum temperature. Data was downloaded through FTP using the R package 'prism' (Hart and Bell, 2015). Since the model doesn't differentiate between rain and snow, we assumed that all precipitation fell as snow below a threshold of 1.5° C, and as rain above this threshold. This threshold is near the upper bound of the transition temperature across non-alpine North America found in the study by Jennings et al. (2018).

2.3 Analysis Methods

Daily input data were aggregated spatially and temporally to classify years as "warm" or "cool", to analyze changes in snowpack and streamflow, and compute basin-wide water budgets. First, we developed a multimetric analysis of the GHCN temperature data to classify years into "warm" and "cool" relative to the mean for the 14-year period. Then, using these yearly classifications, SNODAS snow and USGS streamflow data were analyzed within each year type to evaluate differences in melt and streamflow amounts and timing. The melt estimates from SNODAS were used in conjunction with the streamflow data to evaluate hydrologic effects of melt changes. Statistics of seasonal flow timing and amount were extracted from the daily gauge data across the basin. These streamflow data were then compared to SNODAS output and precipitation data from PRISM to examine seasonal net recharge associated with melt. All of the data analysis techniques were performed in R.

2.3.1 Spatial Aggregation

Several spatial aggregations were employed during the analyses. The GHCN station data were aggregated over HUC-8 basins to provide complete spatial coverage of the state and allow temperature variation among basins. The SNODAS spatial data were imported as raster files into the statistical software R (R Core Team, 2019) and then mean daily melt/SWE values were extracted across stream basin polygons, which were calculated for each USGS gauge station using 30 meter (1 arc second) National Elevations Dataset DEM data. The DEM-based stream basin polygons were used for this analysis to relate streamflow to the snowmelt and precipitation inputs over each basin. These spatial aggregates across basins were then viewed through the lens of the three broader regions of the state (SLP, NLP and UP), which are used to analyze melt, streamflow and net recharge.

2.3.2 Multimetric "Warm" and "Cool" Year Classification

We developed a multimetric classification of winter/spring air temperatures as "warm" or "cool" to go beyond simple seasonal average temperatures typically used. We first aggregated the station data spatially, computing daily average air temperatures within HUC-8 basins (see Fig. 1). Hydrologic Unit Code (HUC) basins are drainage basins delineated as part of the "Hydrologic Unit Maps" project of the USGS, ranging from the largest two digit HUC's (HUC-2's) to the smallest 12 digit basins (HUC-12's) (Seaber et al., 1987; USGS, 2014). HUC-8 basins were used to group stations because they offer complete coverage of the state without any overlap, generally include one or more temperature stations, and are sufficiently small to not obscure smaller-scale variations in temperatures. Within each basin, we then computed water-year values for six air temperature metrics: 1) average from October-May; 2) minimum for the same period; 3) winter (Dec-Feb) average and 4) winter minimum; 5) spring (Mar-May) average, and 6) spring minimum. These metrics were chosen because temperature changes have been found to be the primary driver for changing snowmelt dynamics (Boyer et al., 2010; Cline, 1997; Hamlet et al., 2005; Hodgkins and Dudley, 2006a, 2006b; Hodgkins et al., 2007; Jefferson et al., 2008; Johnson and Stefan, 2006; McCabe and Wolock, 2010; Mote, 2003; Stewart et al., 2004). We sought to include metrics that would capture whole-season temperatures, equally and separately weighting both winter and spring portions. Minimum temperatures were included because if the nighttime air temperatures stay above the melting temperature the snowpack continues to melt rather than refreeze; minimum temperatures below freezing would delay melting the following day as warmer daytime temperatures must reheat the snowpack until an isothermal snowpack temperature gradient can be reached to generate melt (Cline, 1997).

"Warm" and "cool" year classifications were then determined from multimetric z-scores. Each metric's z-score was calculated by subtracting the yearly mean and dividing by the 14-year standard deviation within HUC-8 basins. The arithmetic mean of the six resultant single metric z-scores (each centered around 0) was then calculated to provide a single annual multimetric score for each HUC-8 (Supplementary Figure 1). An overall annual state metric score was then calculated as the mean across all HUC-8 basins. More positive values for this overall annual score indicate warmer winters than the 14-year norm, and negative values thus indicate cooler. Water years with multimetric scores less than -0.5 were classified as "cool" and greater than 0.5 were classified as "warm". Metric scores between -0.5 and +0.5 were deemed "normal" years. For an individual metric, the 0.5 threshold represents 0.5 standard deviations away from the mean; for the multimetric score the values have a similar meaning though they are not precisely defined as standard deviations above or below the norm. These classifications were then used as the basis for the remainder of the analysis in this study.

2.3.3 Regional-Scale Snowpack and Streamflow Analyses

After classifying each year in the study period as warm, cool or normal the SNODAS data were analyzed within each of our three regions (UP, NLP, and SLP) for changes to melt amount and timing. Daily mean SWE and mean melt output were averaged across grid cells within each of the three regional polygons. Then, annual values for the following statistics were calculated for each region: peak melt/SWE amount, peak melt/SWE timing, number of bare ground days, annual melt amount, 50^{th} quantile of seasonal melt volume (SM50), number of melt events (defined here as periods of consecutive days with melt generated from the snowpack), melt event length and amount, and number of complete melt events (defined as melt events that ended with no remaining snowpack). We then computed arithmetic means of each of these statistics within warm and cool year types.

We also computed warm and cool year average daily time-series SWE curves within each region. These were calculated as the average day-of-water-year SWE within each regional polygon for each year type. This provided an informative visualization of the general snowpack progression through the season, and illustrates both regional and year type differences within the snowpack.

We examined the distribution of the data using several different methods. Most figures of amounts and timing across station/gage data were plotted as violin plots; these plots display y-axis values similar to a standard boxplot, but also display the density of data around a given y-axis value as a vertically-mirrored kernel density estimate. This shows the distribution of data along with the quantiles. Finally, we compared year type distributions using two statistical tests described below.

Stream gauge data were analyzed in a similar manner as the SNODAS output. Since these gauges provide point data that are associated with individual drainage basins for each gauge, there was no need for any spatial aggregation. For each gauge site, statistics were calculated for: winter season peak flow amount and timing, annual flow quantiles, and basin yields. Basin yield is defined as the daily streamflow divided by gauge basin area. Values were then averaged across all gauge basins within each of the three regions. Similar to the snowpack time-series SWE curves, we computed a mean basin yield hydrograph across regions within warm and cool years. From these, we then computed the center of volume (CV), defined as the date of arrival of 50% of the flow between October and May.

2.3.4 Winter and Spring Net Recharge Analysis

Within each stream gauge basin we computed the daily overall basin water balance. This water balance allowed us to estimate net winter and spring recharge (i.e. the net change in storage). Assuming there is minimal evapotranspiration between December and April (Kirchner and Allen, 2020; Supplementary Fig. 2), and that streamflow is the only significant basin outlet (i.e., pumping or losses to deeper geologic units are minimal) the water balance for each gauge basin can be written as

$$\Delta S = P + M - Q \qquad \text{Equation 1}$$

where ΔS is the change in groundwater storage (i.e., net recharge, mm/d), P is rain (mm/d), M is snowmelt (mm/d) and, Q is stream discharge expressed as daily basin yield (mm/d). Rainfall was computed from PRISM precipitation as described above, and daily snowpack basal melt data were extracted from SNODAS to quantify total available liquid water ($P + M$). Daily averages across grid cells for PRISM and SNODAS were calculated within each stream gauge basin. To reduce noise, these daily values were then summed monthly, and medians of the monthly sums was calculated across regions and year types.

2.3.5 Dataset Distribution Tests

Two statistical tests were used to evaluate if data and calculated values from warm years were statistically different from those in cool years. First, annual basin values such as total seasonal melt, the timing of peak SWE, total rain and peak basin yield were calculated. These annual datasets were classified by their year type, and then warm and cool year distributions were evaluated for normality using the Shapiro-Wilk Normality Test (Royston, 1995). These year type data were then compared using both the two-sample Mann-Whitney (Wilcoxon) ranked sum test (Hollander and Wolfe, 1973) and the two-sample Kolmogorov-Smirnov (KS) test (Conover, 1971). The p-values for these two tests were evaluated on a 95% confidence threshold to evaluate if the two year-type datasets were statistically different.

3. Results

3.1 Warm and Cool Year Classification

Four years were classified as "warm" (2004, 2010, 2012, 2017) and five years as "cool" (2008, 2011, 2013, 2014, 2015) using the multimetric analysis. The spatial distribution of metric scores is generally uniform (Fig. 2) across the study area. In particular, spatial homogeneity increases as metric scores deviate from 0. A visual examination of the metric score distribution does not reveal any temporal trends, with the coldest year (2014) and warmest year (2012) occurring within a short timeframe. Nor does the relatively short study period provide a long enough timeframe to robustly assess trends.

The influence of the individual metrics on the overall metric score was examined by comparing time series of the individual metric scores averaged across all HUC-8 basins in the study area (Supplementary Fig. 1). While there was deviation from the overall metric score for some metrics, rarely did individual metrics classify years differently from the overall metric. The average spring temperature and minimum spring temperature metrics classified the year as cooler than the overall metric two and three times respectively. The winter average and minimum temperature metrics only classified a year as cooler than the overall metric once.

3.2 Precipitation Analysis

Using the K-S test on the PRISM data, we examined if the hydrologic differences between year types were driven by changes in total precipitation (both solid and liquid) amounts rather than changes to snowmelt regimes. The K-S test was run on total precipitation as well as each of the precipitation types individually comparing warm year precipitation totals to cool year totals. Gridded total precipitation across the study region showed significant differences between cold and warm winters ($P<0.001$), with warm winters having an average of 356 mm and cool years 419 mm. While both snow and rain distributions between the two year types have P-values below 1% ($P < 0.001$ and $P = 0.008$, respectively).

3.3 Snowpack Analysis

Snow in all regions generally starts to accumulate in late November (around the 50^{th} day of the water year, Figure 3), with the UP receiving its first snow on average 21 days before the Southern Lower Peninsula (SLP). Cooler winters have consistently higher SWE regardless of the region or time of year, and the persistence of the snowpack is significantly longer. In both year types, snow persists significantly longer in the UP than in either the Northern or Southern LP (on average lasting 17 and 20 days longer than snow in the Northern LP in warm and cool years respectively). Across regions and year types average peak SWE occurs in a 6-week window, ranging from January 28-March 9. Snow amounts increase moving northward for all year types, with the UP's maximum SWE on average about 100 mm higher than the SLP maximum SWE (Figure 3, Table 1). Note that snowpack SWE variability is highest between days 160 and 200 (mid-March to late April).

These regional differences that are independent of year type also appear in the total seasonal melt within HUC-8 basins, with those in the UP experiencing nearly double the amount of melt as the SLP in both year types (Figure 4). These regional differences are also reflected in winter bare ground days (Table 1). In all year types, the UP has fewer bare ground days, correlating with fewer complete melt events. The SLP has the most bare ground days regardless of year type, while the NLP falls between the two. The snowpack in the UP melts in fewer melt events than the more southern regions, and relative to the SLP, most of those melts do not continue to complete melt of the snowpack. The NLP shows differences and similarities to the other two regions, having similar numbers of melt events per season as the UP, but more of those melt events continue to completion, similar to what's seen in the SLP.

More melt is produced (and thus more snowfall occurred) in cool years regardless of region, with cool years producing around 100 mm more melt in all regions (Table 1). The Mann-Whitney ranked sum test on annual basin melt totals grouped by year type showed a significant difference between melt in the two different year types with a $p < 0.0001$ (Table 4). Cool years have more total melt events but fewer that go to completion where no snow is left on the ground (Figure 4, Table 1). In warm years in all regions the timing of peak melt closely correlates with the timing of 50% of seasonal melt, but in cool years, peak melt occurs several weeks before this date.

Regionally these year type differences are greater in magnitude in the UP and SLP. These two northern and southern regions show the most significant differences in snowfall and snowmelt between year types, while the year type differences in the NLP are less significant (Table 4). The distribution of snow-related values between warm and cool years is significantly different with a 95% confidence interval in all regions except the NLP, which had p-values below this confidence interval for peak melt amount and timing, maximum SWE timing and the timing of 50% of bulk seasonal melt (Table 4). In the UP, only two values were not statistically different according to the ranked sum test: total seasonal melt ($p = 0.15$) and season length ($p = 0.077$). In the SLP only one metric scored below the confidence interval threshold: peak melt time ($p = 0.13$). When comparing state-wide distributions between year types all values were significantly different for both tests.

While the SLP and UP snow datasets both show different distributions between year types, the way those datasets differ depends on the region. During the onset of winter in October-December, the SLP snowpack shows similar patterns in both warm and cool years, but these differences increase as the season progresses (Figure 3). The median day of peak melt in the SLP is approximately 19 days earlier in cool years, but it is 43 days earlier in warm years in the UP (Table 1). It must be noted that this may be influenced by the small number of years in the study period.

3.4 Streamflow Analysis

Similar to the snowmelt results, the differences between year types is largest in the SLP and UP (Figure 5, Table 4). The timing of the peak regional basin yield is earlier in all regions in warm years compared to cool years, ranging from one day earlier in the SLP to 36 days earlier in the UP. The center of volume timing is also earlier in warmer winters in all regions, most notably 30 days earlier than in the UP. The UP's peak basin yield in cool years is twice that of peak yield in warm years (3.0 vs. 1.6 mm/day), but in the SLP, year type peak yield are similar with a difference of only 2.0 mm/day. Cool years produced more total seasonal basin yield in all regions, but the difference is only large in the UP.

Regional differences within year types are more noticeable in cool years. Peak basin yield in cool years increases northward, correlating with more melt ranging from 2.0 mm in the SLP to 2.0 mm in the UP. In warm years these regional differences are muted, with the peak basin yield increasing southwards in warm years, from 1.6 mm in the UP to 2.2 mm in the SLP (Table 2). The results from streamflow in the NLP don't show as clearly defined a trend, with the NLP having the highest total basin yield amounts across regions in all year types, but the lowest peak basin yield amounts.

Once again, the lack of difference between year type datasets in the NLP is reflected in the results of the statistical tests run on the data distributions. Across the entire state, warm and cool year total seasonal basin yield, peak basin yield amount and timing, and the timing of 50% of seasonal cumulative flow (BY50) are all significantly different using a 95% confidence interval threshold for both the ranked sum test and the KS test (Table 4). Similarly, when examining the SLP and UP these basin yield datasets are all significantly different for both tests using this threshold. However, the NLP falls below the confidence interval in BY50 (ranked sum $p = 0.32$; KS $p = 0.30$), total seasonal basin yield (KS $p =$ o.22) and peak basin yield timing (ranked sum $p = 0.60$).

3.5 Winter and Spring Recharge Analysis

Net groundwater recharge (from Equation 1) monthly values across regions and year types show striking patterns (Fig. 6). There were significant variations in net groundwater recharge estimates by region. Groundwater storage decreased in midwinter when basin yield totals exceeded total precipitation inputs. There was more net recharge in warm years than in cool years for most months in all regions, particularly for the SLP which had on average 19 mm more net recharge in warm years. Across the entire state, as well as each region individually, the distribution of basin net recharge values between year types is statistically significant at the 95% confidence level for both tests (Table 4).

Unlike differences in snowpack, during the deeper winter months the UP shows the least difference between year types, while the net recharge in the Lower Peninsula can be centimeters more in warm years. Cool year net recharge for April within both the NLP and UP increases substantially in response to more melt from the persistent snowpack. This is reflected in the region's very high S/P ratio in cool years (Table 3). Peak monthly net recharge amounts give insight to recharge mechanics in the different regions, with the peak monthly net recharge in the UP making up the majority of the season's total net recharge (79% in cool years and 57% in warm years), while the peak monthly contribution to net recharge decreases southward. In the NLP, the peak monthly net recharge contributed to 64% of the seasonal total net recharge in cool years and 48% in warm years; for the SLP it was 31% in cool years and 32% in warm years. Regional recharge amounts may also be influenced by the amount of liquid precipitation, with higher total net recharge in the SLP correlating with higher rain amounts. Net recharge in the NLP, similar to streamflow differences, has less clear year type differences with total recharge similar in both warm and cool years despite differences in total rain and S/P, indicating the surficial geology's role affecting recharge and not just melt/rain amounts. The deep surficial deposits with very high sand content leading to relatively high soil hydraulic conductivity values (2 to 10 mm/day for much of the NLP) could contribute to the lack of difference seen in streamflow and net recharge in different year types (Fig. 1). Net recharge is higher in the Lower Peninsula than in the UP for much of the year, in all year types. This is likely related to more liquid winter precipitation in the southern regions.

4. Discussion

Our analyses support all four study hypotheses: 1) snow melt occurred earlier, and in lower quantities, in all regions during warm years; 2) complete melt events occurred more frequently in warmer years, leading to more days without snow on the ground; 3) basin yield (and thus stream discharge) peaked earlier and lower during warm year winters and finally; 4) there is more net groundwater recharge during warm years in the southern LP, but not in the UP. We also found that differences between warm and cool years were highest in the North and decreasing to the South.

Average snowpack SWE peaks lower in warm years, with earlier melting of the snowpack (Fig. 3). This difference between SWE peaks across year types is more notable in the northern regions, likely due to the greater snowfall amounts these areas receive. Warmer years also produce less snowmelt, and thus a smaller snowmelt component of watershed hydrologic fluxes (Fig. 4). How and when this melting occurs is also noticeably different between year types. Warm and cool years had similar numbers of melt events in all regions, but more of those melts are progressing to completion in warm years. The average melt event length and amount are less in warm years than cool years, especially in the UP. So while there may be similar numbers of melt events in both year types, the snowpack is less persistent throughout the season in warm years and melts more quickly. Indeed, for the UP there are 40 more bare ground days in warm years, indicating substantial portions of the season without snow cover, corresponding with increased melt events and complete melts. This differs from recent findings of Musselman et al. (2017) who indicated that warmer climate produces slower melt rates because more melt is occurring earlier in the year when days are shorter and the solar declination is lower. However, that study focused on thicker snowpacks in the western United States located at higher elevations which persist later into the spring, and as a result may be more sensitive to such climatic changes.

Another facet of the changing snowpack dynamics is the response of Lake Effect snow amounts to climate warming. Burnett et al. (2003) found that warming temperatures in response to global climate change may be driving higher Lake Effect snow totals as the warmer temperatures lead to less ice cover and higher evaporation rates. Even with possibly increased amounts of evaporation from the Great Lakes under warmer temperatures, those same warmer temperatures are likely to lead to more of that Lake Effect precipitation occurring as rain rather than snow during the winter months (Champagne et al., 2020; Hayhoe et al., 2010). While snow amounts may be increasing through the decades, this study’s short temporal window is unlikely to capture such climatic influences. Furthermore, the complex interactions of atmospheric oscillation indices, rising global temperatures and local variations in wind, humidity and other factors contributing to the Lake Effect phenomena is beyond the scope of this study.

Streamflow, especially in the northern regions, responds dramatically to changing snowmelt in warm years. Streamflow patterns are responsive to earlier melting in warm years. Basin yields were lower and peaked much earlier in warm years, correlating with the earlier peak melt events in these years. These results also agree with what many studies of changes to snowmelt hydrology under warming climate scenarios have found (Boyer et al., 2010; Campbell et al., 2011; Hodgkins et al., 2003; Hodgkins and Dudley, 2006b; Johnston and Shmagin, 2008; Novotny and Stefan, 2007; Stewart et al., 2004).

The influence of landcover on basin yield should also be considered in further studies to help elucidate regional differences in surface flows. For instance, the more urbanized southern regions may show less difference between warm and cool year flows because no matter when melting occurs, much of that melt will become overland flow on the more extensive impermeable surfaces. However, the role of land cover in these results is likely limited, as urban areas are generally limited (except in the SLP) and tend to be located lower within watersheds with most differences attributed to latitudinal climate gradients including significantly lower annual snowfall in the south, which leads to more intermittent snow cover. This also agrees with the results from Huntington et al. (2004), who found that the more northern New England study sites are likely to experience the most significant downward trends in snow to precipitation ratio (S/P) and earlier peak flows. The downstream effects of these streamflow changes are not entirely understood, and lake level differences between years should be further examined in future research since streams contribute close to half of the water stored in the lakes, and lake levels have been projected to decline with warmer temperatures (Angel and Kunkel, 2010; Mortsch et al., 2000).

Net recharge to shallow groundwater peaked earlier in warm years and exceeded the cool year net recharge in the southern regions. In warm years, the highest amount of net recharge occurs in March, a month earlier than in cool years. Indeed, the effect may be greater than calculated here, because some plants are already starting to exit their dormant phase in April, particularly in warm years. While we have assumed that winter ET rates are negligible for

Equation 1, significant ET during April of warm years would reduce net recharge and make the shift in recharge timing even more pronounced. Kirchner and Allen (2020) determined from end-member “splitting” analysis of experimental data collected at the Hubbard Brooks Experimental Forest in New England estimated that little to no ET originated from snow season (Dec-Mar) precipitation (15 ± 15%). Using NLDAS-2 forcing data, we calculated average potential evapotranspiration (PET) for Michigan from November-April for the study years, finding the winter PET for the majority of the state totals around only 10 mm (Xia, Y., 2012; Supplementary Fig. 2). Regardless of ET effects, by the end of April warm years still show higher overall net recharge than cool years in the southern LP, tentatively confirming the hypothesis of increased recharge in warm years. However, the hydrologic pathways for recharge to shallow groundwater are complex, and thus process-based modeling will be needed to fully evaluate these processes. The cause of this increased recharge is currently unclear and is further complicated due to the influence of frozen soil on infiltration rates. Several studies have shown that reduced snow depth and days with snow on the ground decrease thermal insulation of soil moisture, leading to more frozen ground and reduced infiltration into the soil (Isard and Schaetzl, 1998; Iwata et al., 2011).

Despite the increased likelihood of frozen soil in warmer years, there appears to be more net recharge in such years in the south. This could be due to preferential flow paths through and around frozen soils developing like those found by Mohammed et al. (2019) in the Canadian prairies, or it could be due to climatological and geological differences between regions. Regional differences similar to those found in the melt and basin yield results are present in net recharge estimates as well, with the southernmost region showing the least difference between year types. A number of potential mechanisms may produce these regional differences. For example, the general hydrologic processes governing runoff generation may be affecting how much melt infiltrates the subsurface instead of contributing to surface flows. Shallower snow depths that intermittently melt may allow proportionally more percolation to the water table compared to large melts that cause soil saturation early in the melt leading to overland flow. This may be part of the reason that the NLP had little difference in peak streamflow and center of volume arrival time; soils there are fairly uniformly sandy and coarse-textured with high hydraulic conductivity, compared to those of the SLP and UP (Fig. 1; Soil Survey Staff, 2020). Mean hydraulic conductivity for the NLP is 2200 mm/day, compared to an average of 1000 mm/day for both the SLP and UP soils. Increased rain-on-snow events may also increase recharge as the warmer rain could increase the soil moisture temperature. In addition, more melt occurs in the late winter and early spring months in warmer years long before plants are active. Regional differences in melt and basin yield amounts also likely affect recharge. Again, due to the complex interplay of physical processes, process-based integrated hydrologic modeling of recharge is necessary improve the understanding of such relationships.

Regardless of the drivers of these regional differences, there appears to be a latitudinal transition zone across the state, with the regions north of the transition zone (the UP) showing more pronounced differences in snow hydrology between year types than the southern regions. The exception is total annual melt, for which all regions showed less melt (and correspondingly less snowfall) during warm years. The lack of difference between streamflow and recharge during warm and cool years in the south is likely because these regions receive less snow than the northern parts of the state. When examining the distributions of year type datasets regionally, the NLP appears to be the transition zone as it is the only region to consistently fall below the 95% confidence interval using both statistical tests (Table 4). This transition zone may represent a latitudinal gradient south of which receives too little annual snow for large timing shifts and north of which warming has very distinct melt effects. Thus, changes to snowmelt hydrology resulting from a warming climate aren't as impactful to the overall water budget in these transitional regions. The more northern region showing a larger difference between year types is similar to findings by Suriano et al. (2019) who found that from 1960-2009 snow depth amounts across the Great Lakes Basin declined by approximately 25%, with the most significant decreases in the northern areas of the basin. An alternative explanation is that the global climate hasn't yet warmed sufficiently to impact the hydrology of the northern regions in cool winters as it has the south. To confirm this, study of longer-term trends is needed to establish the location and stationarity of this transition as the climate continues to warm.

5. Conclusions

Using observations from GHCN and the USGS, alongside model reanalyses from SNODAS and PRISM, this study found that Michigan's snowmelt hydrology shifts significantly between years defined as "warm" and "cool", with the degree of shift varying by region. In all regions, warm years had less total snowmelt with earlier melt occurring in more complete events than cool years. As expected, precipitation also shifted towards more rain in warm years. These changes to melt and precipitation caused earlier and lower peak streamflows in warm years, with less groundwater recharge. Differences between regions indicate a "transition zone" where southern regions show smaller differences between warm and cool years.

Future studies will focus on expanding the spatial and temporal scope of this research. The most significant limitation in this study was the short timeframe available from the snow model. To look further back in time, the only source of empirical climate data is historical weather data, which has spatial limitations and only provides snowfall/snow depth data without the SWE component. Historical climate model outputs are available, but they either don't include the SWE component or are too coarse in their spatial resolution. By using the metrics defined here, the multimetric analysis can be applied to years over a longer period to robustly classify warm versus cool years. Then using this multimetric analysis with stream gauge records for those expanded years, inferences about melt processes can be made without having actual melt data—which are generally poorly available prior to SNODAS. We plan to apply this process across larger scales to better understand how widespread these hydrologic changes may be. Ultimately the results of this and future work will form an observational foundation for targeted and improved simulations of these melt processes to quantify how winter and spring hydrology in the Great Lakes will likely change in the coming decades due to global change.

6. Additional Information and Declarations: Code Availability

Code used in the analyses performed in this research are available at the Consortium of Universities for the Advancement of Hydrologic Science, Inc. (CUAHSI) HydroShare at https://www.hydroshare.org/resource/39b0d20939df4b72b2fd1fa05a8fc99b/ (https://doi.org/10.4211/hs.39b0d20939df4b72b2fd1fa05a8fc99b). HydroShare is a web based system for sharing hydrologic data, code and models between hydrologic researchers. The code found on HydroShare and producing the results for this manuscript used several key packages. Downloading of data from various sources relied on the "dataRetrieval" (De Cicco, et al., 2018), "prism" (Hart and Bell, 2015), and "rnoaa" (Chamberlain, 2020) packages. Spatial mapping and aggregation of data was completed using the "grid" (R Core Team, 2019), "raster" (Hijmans, 2020), "rgdal" (Bivand, R. et al., 2019), "rgeos" (Bivand and Rundel, 2019) and "sp" (Pebesma and Bivand, 2005) packages. Analysis of the data was greatly aided by "ddplyr" (Wickham et al., 2020), "lubridate" (Grolemund and Wickham, 2011), "plyr" (Wickham, 2011) and "reshape2" (Wickham, 2007). Finally, graphics plotting was created primarily using the "colorRamps"

(Keitt, 2012), “ggplot2” (Wickham, 2016) and “sp” (Pebesma and Bivand, 2005) packages. This research would not have been possible without the contributions made by the developers of these packages.

Acknowledgements

This research was supported by USDA-NIFA grant 2015-68007-2313, NOAA grant NA12OAR4320071, and NASA grant NNX11AC72G along with Michigan State University’s Environmental Science and Public Policy Program and the Department of Earth and Environmental Sciences. Any opinions, findings, and conclusions or recommendations expressed in this material are those of the authors and do not necessarily reflect the views of USDA NIFA, NASA, or NOAA.

References

Adam, J.C., Hamlet, A.F., Lettenmaier, D.P., 2009. Implications of global climate change for snowmelt hydrology in the twenty-first century, in: Hydrological Processes. pp. 962–972. https://doi.org/10.1002/hyp.7201

Andresen, J.A., 2012. Historical Climate Trends in Michigan and the Great Lakes Region, in: Dietz, T., Bidwell, D. (Eds.), Climate Change in the Great Lakes Region: Navigating an Uncertain Future. Michigan State University Press, East Lansing, Michigan, pp. 17–34.

Angel, J.R., Kunkel, K.E., 2010. The response of Great Lakes water levels to future climate scenarios with an emphasis on Lake Michigan-Huron. J. Great Lakes Res. 36, 51–58. https://doi.org/10.1016/j.jglr.2009.09.006

Argyilan, E.P., Forman, S.L., 2003. Lake Level Response to Seasonal Climatic Variability in the Lake Michigan-Huron System from 1920 to 1995. J. Great Lakes Res. 29, 488–500. https://doi.org/10.1016/S0380-1330(03)70453-5

Arora, V.K., Boer, G.J., 2001. Effects of simulated climate change on the hydrology of major river basins. J. Geophys. Res. 106, 3335–3348. https://doi.org/10.1029/2000JD900620

Barnett, T.P., Adam, J.C., Lettenmaier, D.P., 2005. Potential impacts of a warming climate on water availability in snow-dominated regions. Nature 438, 303–309. https://doi.org/10.1038/nature04141

Barrett, A.P., 2003. National Operational Hydrologic Remote Sensing Center Snow Data Assimilation System (SNODAS) Products at NSIDC. NSIDC Spec. Rep. 11 19.

Berghuijs, W.R., Woods, R. a, Hrachowitz, M., 2014. A precipitation shift from snow towards rain leads to a decrease in streamflow-supplement. Nat. Clim. Chang. 4, 583–586. https://doi.org/10.1038/NCLIMATE2246

Bivand, R., Keitt, T., Rowlingson, B., 2019. rgdal: Bindings for the ‘Geospatial’ Data Abstraction Library. R package version 1.4-8. https://CRAN.R-project.org/package=rgdal

Bivand, R. Rundel, C., 2019. rgeos: Interface to Geometry Engine – Open Source (‘GEOS’). R package version 0.5-2. https://CRAN.R-project.org/package=rgeos

Boyer, C., Chaumont, D., Chartier, I., Roy, A.G., 2010. Impact of climate change on the hydrology of St. Lawrence tributaries. J. Hydrol. 384, 65–83. https://doi.org/10.1016/j.jhydrol.2010.01.011

Brubaker, K.L., Rango, A., 1996. Response of snowmelt hydrology to climate change. Water. Air. Soil Pollut. https://doi.org/10.1007/BF00619293

Burakowski, E.A., Wake, C.P., Braswell, B., Brown, D.P., 2008. Trends in wintertime climate in the northeastern United States: 1965-2005. J. Geophys. Res. Atmos. 113. https://doi.org/10.1029/2008JD009870

Burnett, A.W., Kirby, M.E., Mullins, H.T., Patterson, W.P., 2003. Increasing Great Lake-effect snowfall during the twentieth century: A regional response to global warming? J. Clim. 16, 3535–3542. https://doi.org/10.1175/1520-0442(2003)016<3535:IGLSDT>2.0.CO;2

Byun, K., Hamlet, A.F., 2018. Projected changes in future climate over the Midwest and Great Lakes region using downscaled CMIP5 ensembles. Int. J. Climatol. 38, e531–e553. https://doi.org/10.1002/joc.5388

Campbell, J.L., Driscoll, C.T., Pourmokhtarian, A., Hayhoe, K., 2011. Streamflow responses to past and projected future changes in climate at the Hubbard Brook Experimental Forest, New Hampshire, United States. Water Resour. Res. 47. https://doi.org/10.1029/2010WR009438

Chamberlain, S., 2020. rnoaa: 'NOAA' Weather Data from R. R package version 1.0.0. https://CRAN.R-project.org/package=rnoaa

Champagne, O., Arain, M.A., Coulibaly, P., 2019. Atmospheric circulation amplifies shift of winter streamflow in southern Ontario. J. Hydrol. 578. https://doi.org/10.1016/j.jhydrol.2019.124051

Cherkauer, K.A., Sinha, T., 2010. Hydrologic impacts of projected future climate change in the Lake Michigan region. J. Great Lakes Res. 36, 33–50. https://doi.org/10.1016/j.jglr.2009.11.012

Chin, N., Byun, K., Hamlet, A.F., Cherkauer, K.A., 2018. Assessing potential winter weather response to climate change and implications for tourism in the U.S. Great Lakes and Midwest. J. Hydrol. Reg. Stud. 19, 42–56. https://doi.org/10.1016/j.ejrh.2018.06.005

Clark, M.P., Hendrikx, J., Slater, A.G., Kavetski, D., Anderson, B., Cullen, N.J., Kerr, T., Örn Hreinsson, E., Woods, R.A., 2011. Representing spatial variability of snow water equivalent in hydrologic and land-surface models: A review. Water Resour. Res. 47. https://doi.org/10.1029/2011WR010745

Cline, D.W., 1997. Effect of Seasonality of Snow Accumulation and Melt on Snow Surface Energy Exchanges at a Continental Alpine Site. J. Appl. Meteorol. 36, 32–51. https://doi.org/10.1175/1520-0450(1997)036<0032:EOSOSA>2.0.CO;2

Clow, D.W., 2010. Changes in the timing of snowmelt and streamflow in Colorado: A response to recent warming. J. Clim. 23, 2293–2306. https://doi.org/10.1175/2009JCLI2951.1

Clow, D.W., Nanus, L., Verdin, K.L., Schmidt, J., 2012. Evaluation of SNODAS snow depth and snow water equivalent estimates for the Colorado Rocky Mountains, USA. Hydrol. Process. 26, 2583–2591. https://doi.org/10.1002/hyp.9385

Conover, W.J., 1971. Practical Nonparametric Statistics. New York: John Wiley & Sons, 309-314.

De Cicco, L.A., Hirsch, R.M., Lorenz, D., Watkins, W.D., 2018. dataRetrieval: R packages for discovering and retrieving water data available from Federal hydrologic web services, doi:10.5066/P9X4L3GE

Demaria, E.M.C., Palmer, R.N., Roundy, J.K., 2016. Regional climate change projections of streamflow characteristics in the Northeast and Midwest U.S. J. Hydrol. Reg. Stud. 5, 309–323. https://doi.org/10.1016/j.ejrh.2015.11.007

Dyer, J.L., Mote, T.L., 2006. Spatial variability and trends in observed snow depth over North America. Geophys. Res. Lett. 33. https://doi.org/10.1029/2006GL027258

Farrand, W., & Bell, D. (1982). Quaternary Geology of Michigan. Michigan Department of Natural Resources.

Feng, S., Hu, Q., 2007. Changes in winter snowfall/precipitation ratio in the contiguous United States. J. Geophys. Res. Atmos. 112. https://doi.org/10.1029/2007JD008397

Grolemnund, G., Wickham, H., 2011. Dates and Times Made Easy with lubridate. Journal of Statistical Software, 40(3), 1-25. URL http://www.jstatsoft.org/v40/i03/.

Groundwater Inventory and Mapping Project, 2003. Reference.GSS_SDE_ADMIN.Glacial_Landsystems. Retrieved January 25, 2020 from http://gis-michigan.opendata.arcgis.com/datasets/glacial-landsystems

Hamlet, A.F., Mote, P.W., Clark, M.P., Lettenmaier, D.P., 2005. Effects of temperature and precipitation variability on snowpack trends in the western United States. J. Clim. 18, 4545–4561. https://doi.org/10.1175/JCLI3538.1

Hamlin, Q.F., Kendall, A.D., Martin, S.L., Whitenack, H.D., Roush, J.A., Hannah, B.A., Hyndman, D.W., 2020. Quantifying Landscape Nutrient Inputs With Spatially Explicit Nutrient Source Estimate Maps. J. Geophys. Res. Biogeosciences 125, 1–24. https://doi.org/10.1029/2019JG005134

Hayhoe, K., VanDorn, J., Croley, T., Schlegal, N., Wuebbles, D., 2010. Regional climate change projections for Chicago and the US Great Lakes. J. Great Lakes Res. 36, 7–21. https://doi.org/10.1016/j.jglr.2010.03.012

Hayhoe, K., Wake, C.P., Huntington, T.G., Luo, L., Schwartz, M.D., Sheffield, J., Wood, E., Anderson, B., Bradbury, J., DeGaetano, A., Troy, T.J., Wolfe, D., 2007. Past and future changes in climate and hydrological indicators in the US Northeast. Clim. Dyn. 28, 381–407. https://doi.org/10.1007/s00382-006-0187-8

Hedrick, A., Marshall, H.P., Winstral, A., Elder, K., Yueh, S., Cline, D., 2015. Independent evaluation of the SNODAS snow depth product using regional-scale lidar-derived measurements. Cryosphere 9, 13–23. https://doi.org/10.5194/tc-9-13-2015

Hidalgo, H.G., Das, T., Dettinger, M.D., Cayan, D.R., Pierce, D.W., Barnett, T.P., Bala, G., Mirin, A., Wood, A.W., Bonfils, C., Santer, B.D., Nozawa, T., 2009. Detection and Attribution of Streamflow Timing Changes to Climate Change in the Western United States. J. Clim. 22, 3838–3855. https://doi.org/10.1175/2009JCLI2470.1

Hijmans, R.J., 2020. raster: Geographic Data Analysis and Modeling. R package version 3.1-5. https://CRAN.R-project.org/package=raster

Hodgkins, G.A., Dudley, R.W., Huntington, T.G., 2003. Changes in the timing of high river flows in New England over the 20th Century. J. Hydrol. 278, 244–252. https://doi.org/10.1016/S0022-1694(03)00155-0

Hodgkins, G.A., Dudley, R.W., 2006a. Changes in late-winter snowpack depth, water equivalent, and density in Maine, 1926-2004, in: Hydrological Processes. pp. 741–751. https://doi.org/10.1002/hyp.6111

Hodgkins, G.A., Dudley, R.W., 2006b. Changes in the timing of winter-spring streamflows in eastern North America, 1913-2002. Geophys. Res. Lett. 33. https://doi.org/10.1029/2005GL025593

Hodgkins, G.A., Dudley, R.W., Aichele, S.S., 2007. Historical Changes in Precipitation and Streamflow in the U . S . Great Lakes Basin , 1915 – 2004 Scientific Investigations Report 2007 – 5118, Program.

Hollander, M., Wolfe, D.A., 1973. Nonparametric Statistical Methods. New York: John Wiley & Sons, 68-75.

Homer, C., Huang, C., Yang, L., Wylie, B., Coan, M., 2004. Development of a 2001 national land-cover database for the United States. Photogramm. Eng. Remote Sens. https://doi.org/10.14358/PERS.70.7.829

Homer, C., Dewitz, J., Yang, L., Jin, S., Danielson, P., Xian, G., Coulston, J., Herold, N., Wickham, J., Megown, K., 2015. Completion of the 2011 National Land Cover Database for the coterminous United States – Representing a decade of land cover change information. Photogrammetric Engineering and Remote Sensing. 81, 345-354. https://doi.org/10.14358/PERS.81.5.345

Huntington, T.G., Hodgkins, G.A., Keim, B.D., Dudley, R.W., 2004. Changes in the proportion of precipitation occurring as snow in New England (1949-2000). J. Clim. 17, 2626–2636. https://doi.org/10.1175/1520-0442(2004)017<2626:CITPOP>2.0.CO;2

Isard, S.A., Schaetzl, R.J., 1998. Effects of winter weather conditions on soil freezing in southern Michigan. Phys. Geogr. 19, 71–94.

Iwata, Y., Nemoto, M., Hasegawa, S., Yanai, Y., Kuwao, K., Hirota, T., 2011. Influence of rain, air temperature, and snow cover on subsequent spring-snowmelt infiltration into thin frozen soil layer in northern Japan. J. Hydrol. 401, 165–176. https://doi.org/10.1016/j.jhydrol.2011.02.019

Javed, A., Cheng, V.Y.S., Arhonditsis, G.B., 2019. Detection of spatial and temporal hydro-meteorological trends in Lake Michigan, Lake Huron and Georgian Bay. Aquat. Ecosyst. Heal. Manag. 22, 1–14. https://doi.org/10.1080/14634988.2018.1500850

Jefferson, A., Nolin, A., Lewis, S., Tague, C., 2008. Hydrogeologic controls on streamflow sensitivity to climate variation. Hydrol. Process. 22, 4371–4385. https://doi.org/10.1002/hyp.7041

Jennings, K.S., Winchell, T.S., Livneh, B., Molotch, N.P., 2018. Spatial variation of the rain-snow temperature threshold across the Northern Hemisphere. Nat. Commun. 9, 1–9. https://doi.org/10.1038/s41467-018-03629-7

Johnson, S.L., Stefan, H.G., 2006. Indicators of climate warming in Minnesota: Lake ice covers and snowmelt runoff. Clim. Change 75, 421–453. https://doi.org/10.1007/s10584-006-0356-0

Johnston, C.A., Shmagin, B.A., 2008. Regionalization, seasonality, and trends of streamflow in the US Great Lakes Basin. J. Hydrol. 362, 69–88. https://doi.org/10.1016/j.jhydrol.2008.08.010

Kanno, Y., Letcher, B.H., Hitt, N.P., Boughton, D.A., Wofford, J.E.B., Zipkin, E.F., 2015. Seasonal weather patterns drive population vital rates and persistence in a stream fish. Glob. Chang. Biol. https://doi.org/10.1111/gcb.12837

Keitt, T., 2012. colorRamps: Builds color tables. R package version 2.3. https://CRAN.R-project.org/package=colorRamps

Kirchner, J.W., Allen, S.T., 2020. Seasonal partitioning of precipitation between streamflow and evapotranspiration, inferred from end-member splitting analysis. Hydrol. Earth Syst. Sci. 24, 17–39. https://doi.org/10.5194/hess-24-17-2020

Lilliefors, H.W., 1967. On the Kolmogorov-Smirnov Test for Normality with Mean and Variance Unknown. J. Am. Stat. Assoc. https://doi.org/10.1080/01621459.1967.10482916

McCabe, G.J., Wolock, D.M., 2010. Long-term variability in Northern Hemisphere snow cover and associations with warmer winters. Clim. Change 99, 141–153. https://doi.org/10.1007/s10584-009-9675-2

Menne, M.J., Durre, I., Korzeniewski, B., McNeal, S., Thomas, K., Yin, X., Anthony, S., Ray, R., Vose, R.S., E.Gleason, B., Houston, T.G., 2012. Global Historical Climatology Network - Daily (GHCN-Daily), Version 3 [WWW Document]. NOAA Natl. Clim. Data Cent. https://doi.org/10.7289/V5D21VHZ

Michigan Department of Environment, Great Lakes and Energy (EGLE), 2019. Michigan Quaternary Geology. Available at http://gis-michigan.opendata.arcgis.com/datasets/quaternary-geology-features

Mohammed, A.A., Pavlovskii, I., Cey, E.E., Hayashi, M., 2019. Effects of preferential flow on snowmelt partitioning and groundwater recharge in frozen soils. Hydrol. Earth Syst. Sci. 23, 5017–5031. https://doi.org/10.5194/hess-23-5017-2019

Mortsch, L., Hengeveld, H., Lister, M., Wenger, L., Lofgren, B., Quinn, F., Slivitzky, M., 2000. Climate Change Impacts on the Hydrology of the Great Lakes-St. Lawrence System. Can. Water Resour. J. 25, 153–179. https://doi.org/10.4296/cwrj2502153

Mote, P.W., 2003. Trends in snow water equivalent in the Pacific Northwest and their climatic causes. Geophys. Res. Lett. https://doi.org/10.1029/2003GL017258

Musselman, K.N., Clark, M.P., Liu, C., Ikeda, K., Rasmussen, R., 2017. Slower snowmelt in a warmer world. Nat. Clim. Chang. https://doi.org/10.1038/nclimate3225

National Operational Hydrologic Remote Sensing Center (NOHRSC), 2004. *Snow Data Assimilation System (SNODAS) Data Products at NSIDC, Version 1*. [Snow Water Equivalent, 1 October 2003 to 31 May 2017]. Boulder, Colorado USA. NSIDC: National Snow and Ice Data Center. Doi: Https://doi.org/10.7265/N5TB14TC. [25 September 2017].

Novotny, E. V., Stefan, H.G., 2007. Stream flow in Minnesota: Indicator of climate change. J. Hydrol. 334, 319–333. https://doi.org/10.1016/j.jhydrol.2006.10.011

Peacock, S., 2012. Projected twenty-first-century changes in temperature, precipitation, and snow cover over north america in CCSM4. J. Clim. 25, 4405–4429. https://doi.org/10.1175/JCLI-D-11-00214.1

Pebesma, E.J. Bivand, R.S., 2005. Classes and methods for spatial data in R. R News 5(2), https://cran.r-project.org/doc/Rnews/.

Prism Climate Group, Oregon State University. 2018. Retrieved July 9, 2018, from http://prism.oregonstate.edu

R Core Team. 2019. R: A language and environment for statistical computing. R Foundation for Statistical Computing. Vienna, Austria. https://www.R-project.org/

Royston, P., 1995. Remarik AS R94: A remark on Algorithm AS 181: The W test for normality. Applied Statistics 44, 547-551.

Seaber, P.R., Kapinos, F.P., Knapp, G.L., 1987. Hydrologic Unit Maps (USA). US Geol. Surv. Water-Supply Pap. 2294. https://doi.org/10.3133/wsp2294

Soil Survey Staff, Natural Resources Conservation Service, United States Department of Agriculture. Soil Survey Geographic (SSURGO) Database for CONUS. Available online. Accessed January 25, 2020.

Stewart, I.T., Cayan, D.R., Dettinger, M.D., 2004. Changes in snowmelt runoff timing in western North America under a `business as usual' climate change scenario. Clim. Chang. 62, 217–232. https://doi.org/10.1023/B:CLIM.0000013702.22656.e8

Stottlemyer, R., Toczydlowski, D., 2006. Effect of reduced winter precipitation and increased temperature on watershed solute flux, 1988-2002, Northern Michigan. Biogeochemistry 77, 409–440. https://doi.org/10.1007/s10533-005-1810-1

Suriano, Z.J., Leathers, D.J., 2017. Spatio-temporal variability of Great Lakes basin snow cover ablation events. Hydrol. Process. 31, 4229–4237. https://doi.org/10.1002/hyp.11364

Suriano, Z.J., Robinson, D.A., Leathers, D.J., 2019. Changing snow depth in the Great Lakes basin (USA): Implications and trends. Anthropocene 26, 100208. https://doi.org/10.1016/j.ancene.2019.100208

Tu, J., 2009. Combined impact of climate and land use changes on streamflow and water quality in eastern Massachusetts, USA. J. Hydrol. 379, 268–283. https://doi.org/10.1016/j.jhydrol.2009.10.009

United States Geological Survey (USGS), 2011. NLCD 2011 Land Cover Coterminous United States. Available at https://mrlc.gov/data

United States Geological Survey (USGS), 2014. Watershed Boundary Dataset (ver. USGS Watershed Boundary Dataset: Subbasin (8-digit) 4th level for the entire United States (published 20140311).

United States Geological Survey (USGS), 2018. National Water Information System data available on the World Wide Web (USGS Water Data for the Nation). (n.d.). http://doi.org/http://dx.doi.org/10.5066/F7P55KJN

Wickham, H., 2007. Reshaping Data with the reshape Package. Journal of Statistical Software, 21(12), 1-20. URL http://www.jstatsoft.org/v21/i12/.

Wickham, H., 2011. The Split-Apply-Combine Strategy for Data Analysis. Journal of Statistical Software, 40(1), 1-29. URL http://www.jstatsoft.org/v40/i01/.

Wickham, H., 2016. ggplot2: Elegant Graphics for Data Analysis. Spring-Verlag New York.

Wickham, H., François, R., Henry, L., Müller, K., 2020. dplyr: A Grammar of Data Manipulation. R package version 0.8.5. https://CRAN.R-project.org/package=dplyr

Wolock, D.M., Winter, T.C., McMahon, G., 2004. Delineation and Evaluation of Hydrologic-Landscape Regions in the United States Using Geographic Information System Tools and Multivariate Statistical Analyses. Environ. Manage. https://doi.org/10.1007/s00267-003-5077-9

Xia, Y., Mitchell, K., Ek, M., Sheffield, J., Cosgrove, B., Wood, E., Luo, L., Alonge, C., Wei, H., Meng, J., Livneh, B., Lettenmaier, D., Koren, V., Duan, Q., Mo, K., Fan, Y., Mocko, D., 2012. Continental-scale water and energy flux analysis and validation for the North American Land Data Assimilation System project phase 2 (NLDAS-2): 1. Intercomparison and application of model products. J. Geophys. Res., 117, D03109, doi:10.1029/2011JD016048

Zou, B., Rockne, K.J., Vitousek, S., Noruzoliaee, M., 2018. Ecosystem and transportation infrastructure resilience in the great lakes. Environment 60, 18–31. https://doi.org/10.1080/00139157.2018.1495508

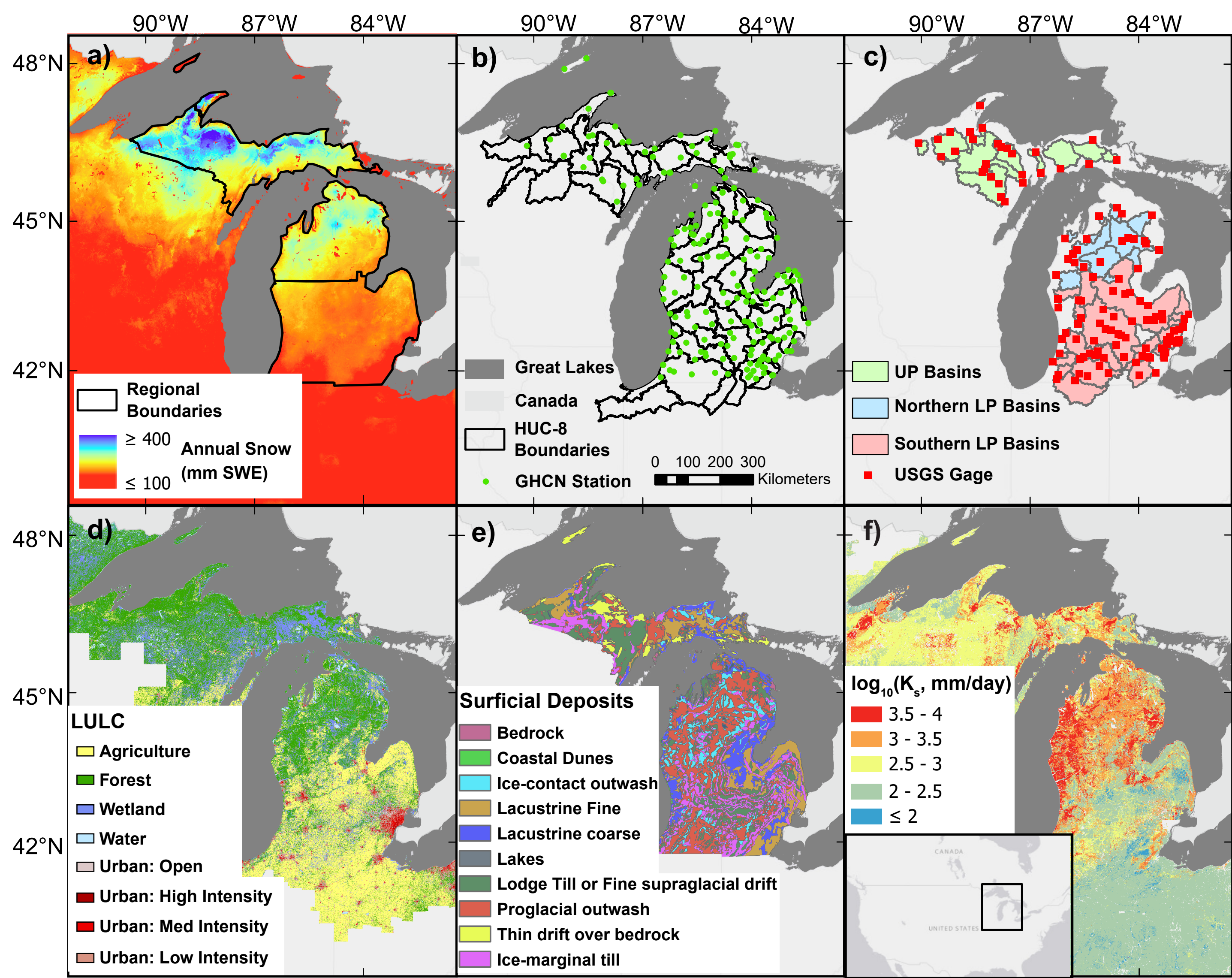
90°W
87°W
84°W
48°N
45°N
42°N
a)
Regional Boundaries
≥ 400
≤ 100
Annual Snow (mm SWE)
b)
Great Lakes
Canada
HUC-8 Boundaries
GHCN Station
0 100 200 300 Kilometers
c)
UP Basins
Northern LP Basins
Southern LP Basins
USGS Gage
d)
LULC
Agriculture
Forest
Wetland
Water
Urban: Open
Urban: High Intensity
Urban: Med Intensity
Urban: Low Intensity
e)
Surficial Deposits
Bedrock
Coastal Dunes
Ice-contact outwash
Lacustrine Fine
Lacustrine coarse
Lakes
Lodge Till or Fine supraglacial drift
Proglacial outwash
Thin drift over bedrock
Ice-marginal till
f)
log10(Ks, mm/day)
3.5 - 4
3 - 3.5
2.5 - 3
2 - 2.5
≤ 2
CANADA
UNITED STATES

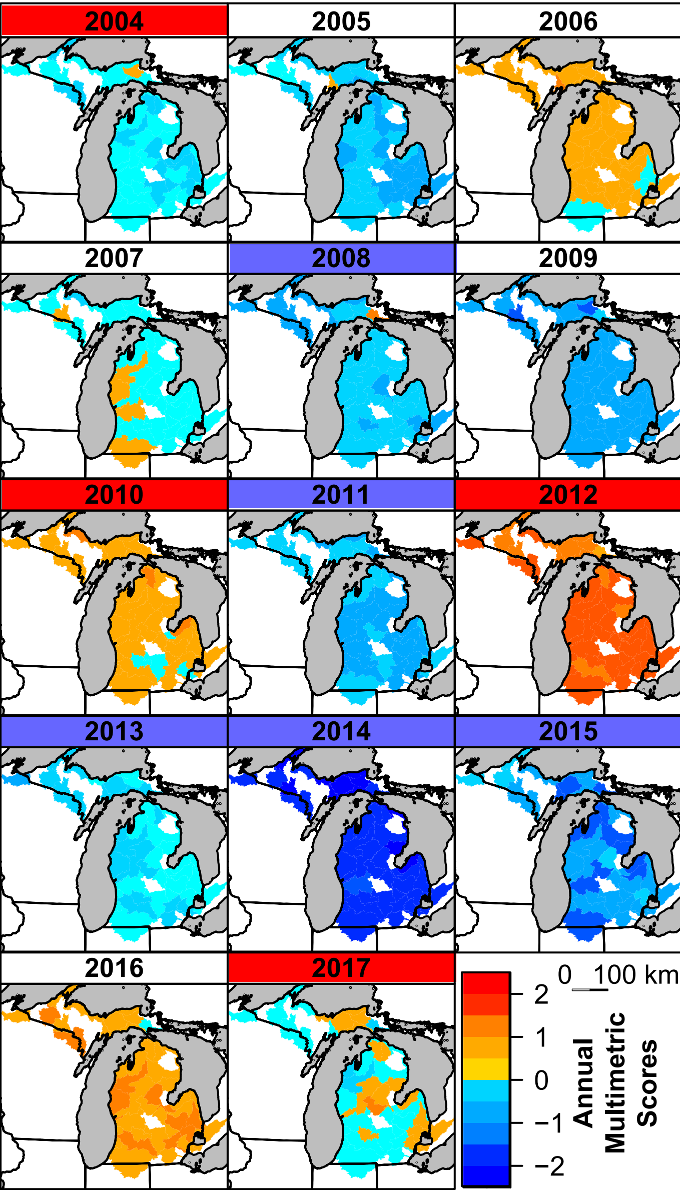
2004
2005
2006
2007
2008
2009
2010
2011
2012
2013
2014
2015
2016
2017
0 100 km
2
1
0
−1
−2
Annual Multimetric Scores

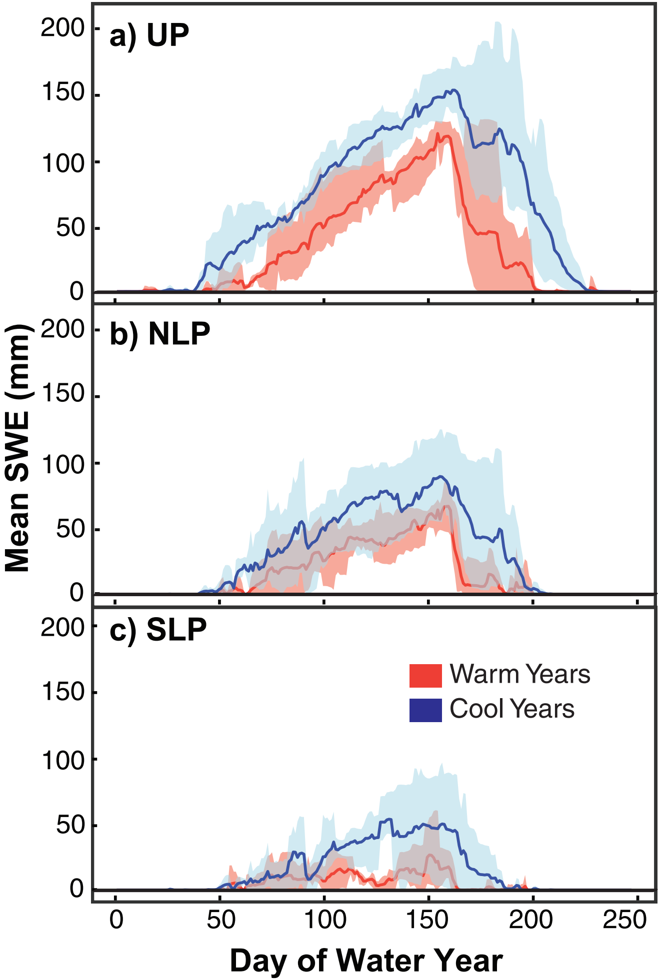
a) UP
b) NLP
c) SLP
Warm Years
Cool Years
Mean SWE (mm)
Day of Water Year
0
50
100
150
200
250

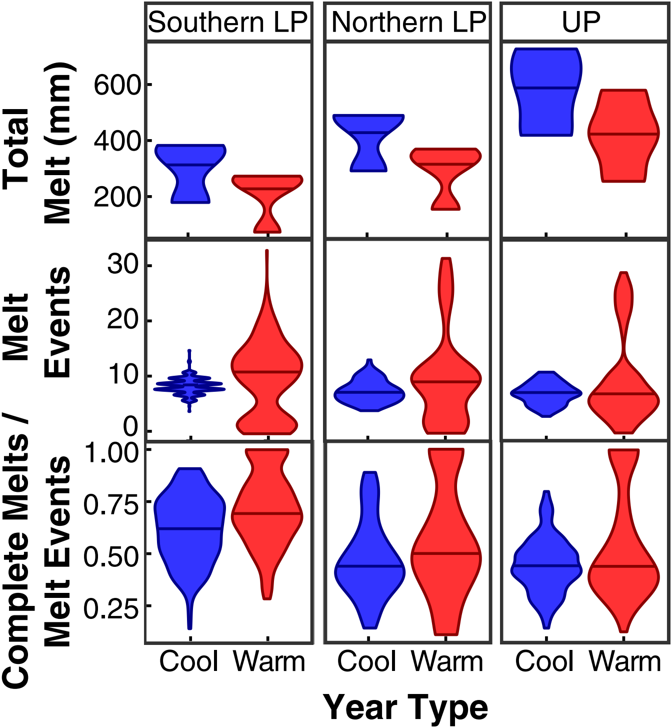
Southern LP
Northern LP
UP
Total Melt (mm)
600
400
200
Melt Events
30
20
10
0
Complete Melts / Melt Events
1.00
0.75
0.50
0.25
Cool
Warm
Cool
Warm
Cool
Warm
Year Type

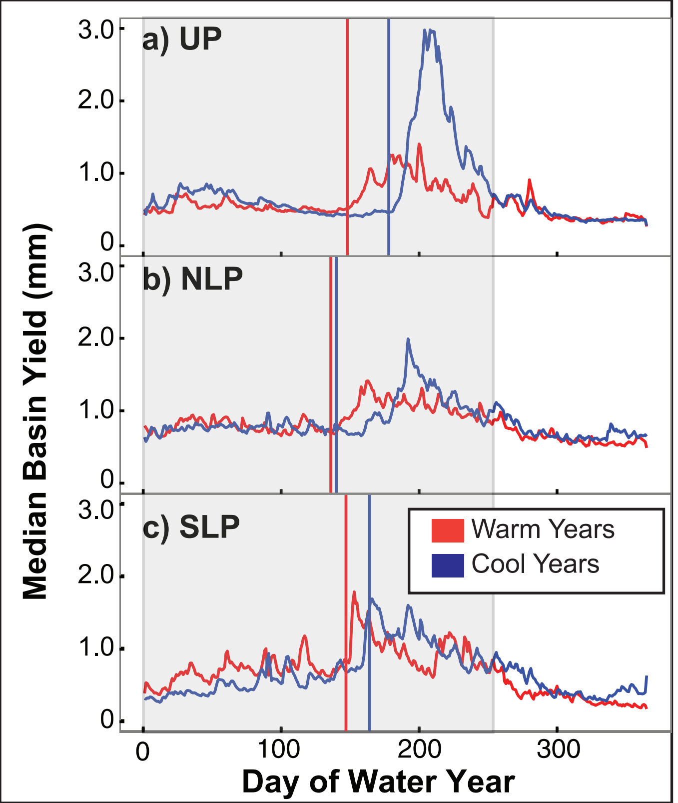

Median Basin Yield (mm)
a) UP
b) NLP
c) SLP
Warm Years
Cool Years
0
1.0
2.0
3.0
0
100
200
300
Day of Water Year

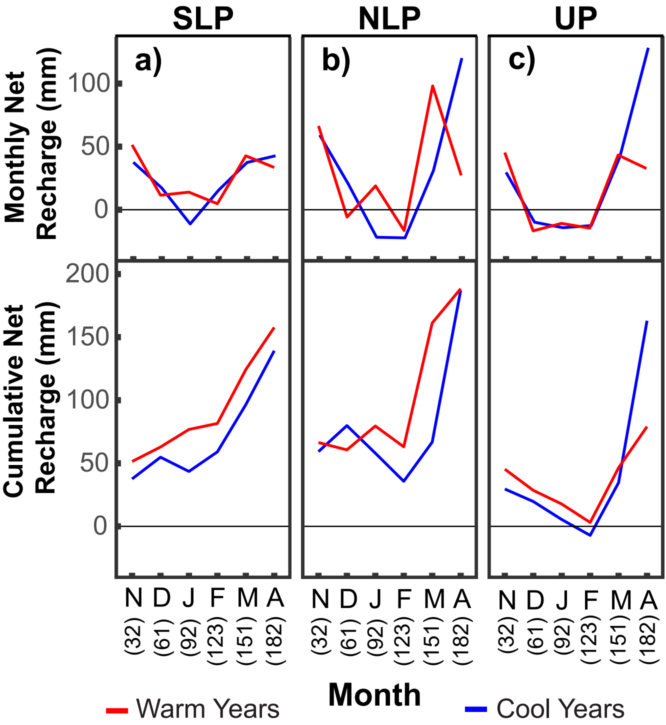
SLP
NLP
UP
a)
b)
c)
Monthly Net Recharge (mm)
Cumulative Net Recharge (mm)
100
50
0
200
150
100
50
0
N (32)
D (61)
J (92)
F (123)
M (151)
A (182)
Month
Warm Years
Cool Years

Region	Southern LP		Northern LP		UP	
Year Type	*Cool*	*Warm*	*Cool*	*Warm*	*Cool*	*Warm*
Peak SWE (mm)	72	35	99	74	167	123
Peak SWE Day of Water Year	132	119	132	147	159	153
Bare Ground Days	128	157	90	135	60	100
Peak Melt (mm)	38	23	38	40	40	29
Peak Melt Day of Water Year	121	140	158	167	217	174
50% Melt Day of Water Year	157	140	177	163	210	180
Total Melt (mm)	304	215	420	296	581	420
Melt Events	9	8	7	8	5	7
Melts to Completion	5	4	2	5	2	4
Melt Event Amount (mm)	24	20	15	10	26	13
Melt Event Length (days)	9	7	10	7	24	10

Region	Southern Lower Peninsula		Northern Lower Peninsula		Upper Peninsula	
Year Type	*Cool*	*Warm*	*Cool*	*Warm*	*Cool*	*Warm*
Total Basin Yield (mm)	200	199	231	222	194	161
Peak Basin Yield (mm)	2.0	2.2	1.6	1.9	3.0	1.6
Peak Basin Yield Day of Water Year	166	165	196	165	205	169
Center of Volume Day of Water Year	164	147	140	136	178	148
Coefficient of Variation (%)	45	39	23	24	69	37

Region	Southern Lower Peninsula		Northern Lower Peninsula		Upper Peninsula	
Year Type	*Cool*	*Warm*	*Cool*	*Warm*	*Cool*	*Warm*
Total Net Recharge (cm)	139	158	187	188	163	79
Peak Monthly Recharge (cm)	43	51	120	98	128	45
Total Rain (cm)	186	233	150	197	53	69
Mean S/P	0.42	0.30	0.58	0.46	0.83	0.68

Variable	Region			
	All	*SLP*	*NLP*	*UP*
Total Melt	<0.001	<0.001	<0.001	*0.2*
Total Basin Yield	<0.001	0.04	*0.3*	0.008
Peak Basin Yield Day of Water Year	<0.001	<0.001	*0.6*	<0.001
BY50 Day of Water Year	<0.001	<0.001	*0.3*	<0.001
Total Net Recharge	0.005	<0.001	0.02	0.02
Max SWE	<0.001	<0.001	<0.001	<0.001
Max SWE Day of Water Year	<0.001	<0.001	*0.9*	<0.001
Total Snow	<0.001	<0.001	<0.001	<0.001
Peak Melt	<0.001	<0.001	*0.8*	0.04
Peak Melt Day of Water Year	0.03	*0.1*	*0.3*	<0.001
SM50 Day of Water Year	<0.001	<0.001	*0.3*	<0.001
Bare Ground Days	<0.001	<0.001	<0.001	<0.001
Season Length	<0.001	<0.001	<0.001	*0.08*